PHYSICAL REVIEW A VOLUME 8, NUMBER 5 NOVEMBER 1973

X-Ray Production by Protons of 2.5–12-MeV Energy*

R. B. Liebert,† T. Zabel, D. Miljanić,‡ H. Larson,§ V. Valković,‖ and G. C. Phillips
T. W. Bonner Nuclear Laboratories, Rice University, Houston, Texas 77001
(Received 19 July 1973)

Characteristic K-shell x-rays produced by proton bombardment of Mn, Fe, Ni, Cu, Zn, Y, Mo, Ag, and Cd targets have been observed for incident energies between 2.5 and 12 MeV. Absolute cross sections for K-shell ionization have been determined and compared to the predictions of the plane-wave Born approximation (PWBA) and binary-encounter approximation (BEA) theories. The (BEA) theory is found to give better agreement at lower bombarding energies and higher Z, while the PWBA fits the data better at lower Z and higher bombarding energies. $L\alpha$, $L\beta$, and $L\gamma$ cross sections for Pb are also presented as a function of energy between 2.5 and 12 MeV.

INTRODUCTION

The development of modern variable-energy accelerators and high-resolution energy-dispersive x-ray detectors has renewed interest in the production mechanisms of charged-particle-induced x-ray emission. The paper of Merzbacher and Lewis[1] summarizes the history of the early x-ray cross-section measurements and shows that a plane-wave Born approximation (PWBA) can reproduce the qualitative behavior of the K-shell electron ionization cross sections as a function of incident energy over more than four orders of magnitude for a wide range of targets. More recently the binary-encounter approximation[2] (BEA) and the impact-parameter approach,[3] among others, have attempted to improve the quantitative agreement of theory with experiment. However, this task is complicated by the fact that most of the older data available were obtained from thick-target yield measurements and only a few targets have been investigated at proton energies above 3 MeV. Table I summarizes the available thin-target data above 2 MeV for the nuclei under study. The aim of the present paper is to provide accurate thin-target K-shell cross sections for a variety of targets at proton energies between 2.5 and 12 MeV.

EXPERIMENT

Targets of Ni, Cu, Fe, Mn, Zn, Y, Mo, Ag, Cd, and Pb were bombarded with 2.5–12-MeV protons produced by the model EN tandem Van de Graaff at Rice University. The experimental apparatus is shown in Fig. 1. The beam entered the scattering chamber after passing through carbon defining slits and was dumped in a magnetically suppressed Faraday cup after passing through the target. X rays were measured at 90° with respect to the incident beam, and a collimator system defining a solid angle of 5.06×10^{-4} sr was provided to minimize in-scattering from areas outside the target beam spot. The count rate measured with no target present was negligible and displayed no peak structure. Polyethylene lining was used on the walls of the chamber to prevent secondary production of x rays in the energy regions being studied, and a magnet surrounding the x-ray collimating slits prevented scattered electrons from producing x rays that could enter the detector.

X rays produced by the proton beams were detected in a 30 $mm^2\times3$ mm Kevex Si(Li) detector. Before entering the crystal, the x rays suffered some attenuation in a 0.0025-cm Mylar chamber window, a 0.32-cm air gap, and a 0.0025-cm Be detector window. The detector output was fed to a pulsed optical-feedback preamplifier and a biased amplifier set to a dynamic range of 3–30 keV.

The beam and target thickness were monitored with a surface-barrier detector mounted at 150° with respect to the beam axis. This counter subtended a solid angle of 1.17×10^{-3} sr and was used to measure the count rate of elastic scattering from each target. The beam current was independently measured by integrating the output of the Faraday cup. The beam integrator's digital output was calibrated to 1% with a standard cell and precision register. Target thicknesses were obtained at 2.5 and 3.0 MeV (where the elastic scattering was assumed to be Rutherford to within 10%) and at other points where reliable elastic scattering data were available. The 3-MeV points were taken before and after the measurement to allow corrections to the data for target-thickness losses. The changes in target thickness during the experiment were less than 8%. The target measurements are summarized in Table II.

The x-ray and particle spectra were collected and stored by the BONER on-line data-collection system used with an IBM 1800 computer. Busy

TABLE I. Summary of proton-induced x-ray-production measurements.[a]

Element	Shell	Energy (MeV)	Target	Reference
Mn	*K*	0.6–6	Foil	10
Fe	*K*	160	Foil	5
		1–3	Foil	9
Ni	*K*	5–28	Foil	4
		1–3	Foil	9
Cu	*K*	160	Foil	5
		1–3	Foil	9
Zn	*K*	0.6–6	Foil	10
Y	No data above 2 MeV			
Mo	*K*	2.4	Thick	6
		160	Foil	5
Ag	*K*	1.7–288	Thick	6
		160	Foil	5
		2–30	Foil	7
		1–3	Foil	9
	L	2–30	Foil	7
Cd	No data above 2 MeV			
Pb	*K*	1.92–288	Thick	6
		160	Foil	5
	L	1.5–425	Thick	8
		1–3	Foil	9

[a] Portions of this table were obtained from Ref. 11.

outputs for the x-ray amplifier and the computer allowed dead-time corrections to be calculated. Pileup losses were kept under 4% by maintaining count rates between 600 and 1000 counts/sec.

Pileup corrections were made by measuring the pileup from a radioactive source as a function of counting rate and x-ray amplifier dead time. These results were used to extrapolate a pileup correction factor for each data point.

The detector efficiency was measured with ^{54}Mn, ^{65}Zn, ^{57}Co, and ^{241}Am sources placed in the target geometry. The ^{241}Am source was fabricated by evaporating a small drop of $Am(NO_3)_3$ solution on a Mylar backing and was calibrated by measurement of the α intensity in a surface-barrier detector of known solid angle. The ^{57}Co source was purchased from Isotope Products Laboratories and was checked against a similar source obtained from and calibrated at Oak Ridge National Laboratory. The ^{54}Mn and ^{65}Zn sources were also obtained from and calibrated at Oak Ridge. Branching ratios were obtained for ^{54}Mn, ^{65}Zn, and ^{241}Am from Ref. 22, and ratios for ^{57}Co from Ref. 23. Corrections were done for self-absorption in the sources and chamber windows. The "intrinsic" efficiency data obtained from factoring out the solid angle is shown in Fig. 2. The data were fitted with a function of the form

$$\epsilon = f_{Be} f_{Au} f_{Si} f_g (1 - f_{CR}),$$

where f_{Be}, f_{Au}, f_{Si} are the transmissions through the Be detector window, the Au electrode layer, and the planar silicon dead layer, respectively.

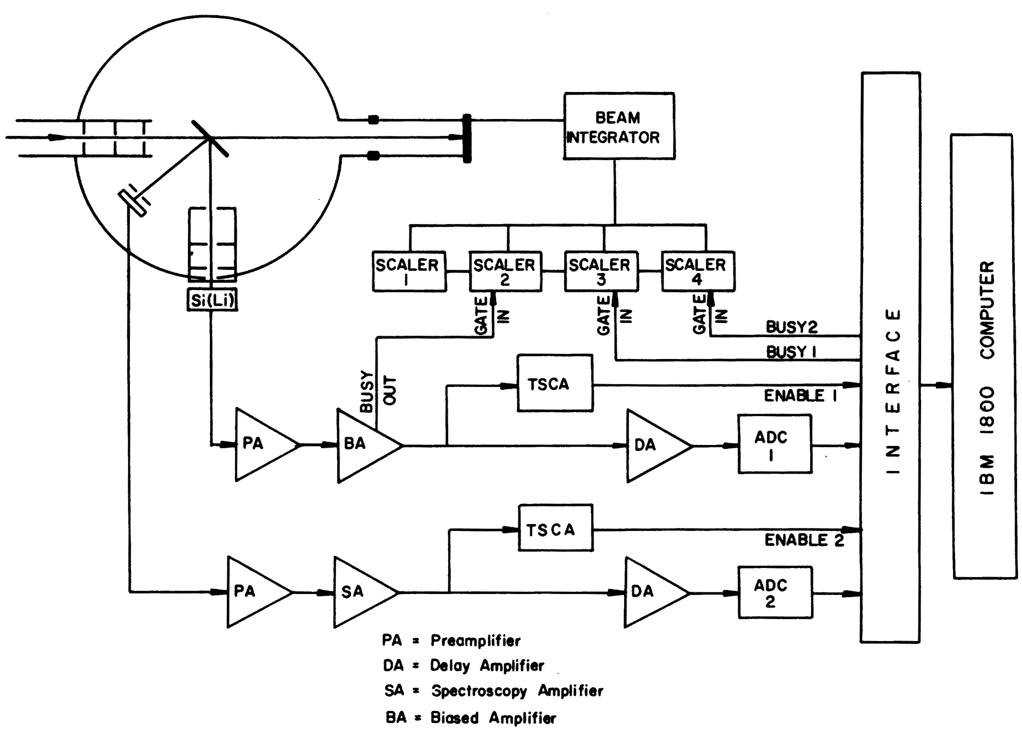

FIG. 1. Experimental apparatus used in the measurements.

TABLE II. Summary of target measurements.

Target [a]	Thickness [b] ($\mu g/cm^2$)	Normalization data	Fluorescence yield [c]
Mn	173.7 ± 17.4 190.8 ± 19.1	Rutherford at 2.5 and 3.0 MeV	0.314 (*K*)
Fe	34.1 ± 3.4 23.2 ± 2.3	Rutherford at 2.5 MeV Ref. 12 at 4, 4.5, and 5 MeV Ref. 13 at 3 MeV	0.347 (*K*)
Ni	248.7 ± 24.9	Rutherford at 2.5 and 3 MeV Refs. 14 and 20 at 6 MeV Ref. 15 at 8 MeV	0.414 (*K*)
Cu	284.4 ± 23.8	Rutherford at 2.5 MeV Ref. 13 at 3 MeV Ref. 16 at 7.8 MeV Ref. 14 at 6 MeV Ref. 17 at 10 MeV	0.445 (*K*)
Zn	180.4 ± 1.6	Rutherford at 2.3 and 3 MeV	0.479 (*K*)
Y	29.3 ± 2.3	Rutherford at 2.5 and 3 MeV Ref. 18 at 6, 6.5, 7, and 9 MeV Ref. 19 at 9 MeV	0.711 (*K*)
Mo	1879 ± 132	Rutherford at 2.5 and 3 MeV Weighing	0.764 (*K*)
Ag	68.3 ± 6.8	Rutherford at 2.5 and 3 MeV	0.830 (*K*)
Cd	606.0 ± 60.6	Rutherford at 2.5 and 3 MeV	0.840 (*K*)
Pb	51.0 ± 2.6	Rutherford at 2.5 and 3 MeV	0.07 (*L*1) 0.363 (*L*2) 0.315 (*L*3)

[a] The Ni and Mo targets were self-supporting. All others were evaporated on 20-μg carbon foils.

[b] Error assignments reflect both the precision of the thickness measurement and the error in the cross sections used for normalization.

[c] Fluorescent yields were obtained from Ref. 21.

f_{CR} is the fraction of the x rays escaping the 3-mm-deep crystal, and f_g is a geometrical factor correcting for losses due to apertures or annular dead areas inside the detector case. The thicknesses of the Au electrode, Si dead layer, and f_g were allowed to vary to fit the eight data points. The χ^2 per degree of freedom was minimized for values of $f_g = 0.88$, $f_{Si} = 1.8$ μm, and $f_{Au} = 32.2$ $\mu g/cm^2$. The value for f_g is consistent with results of subsequent scans of the crystal surface, which showed an abrupt falloff in efficiency near the edge of the detector surface. The values for f_{Si} and f_{Au} cause the efficiency curve to be up to 13% lower than the manufacturer's curves between 5- and 8-keV x-ray energy.

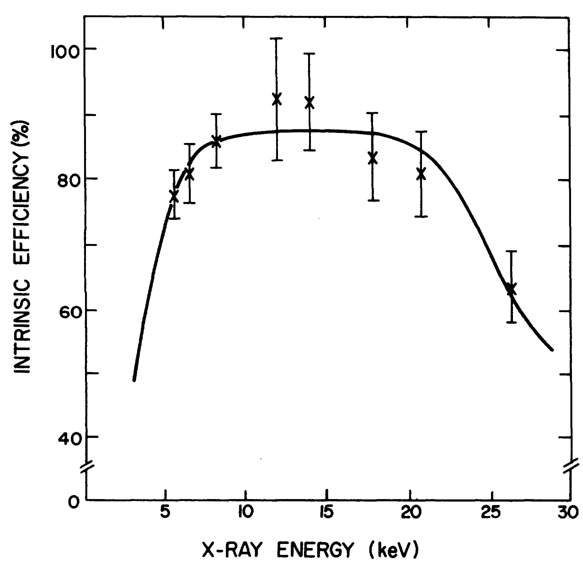

FIG. 2. Si(Li) detector "intrinsic" efficiency data. The solid curve is calculated as the best fit to the data. See text for details.

TABLE III. *K* x-ray-production cross sections (b/sr).[a]

Energy (MeV)	Mn $K\alpha\beta$	Fe $K\alpha\beta$	Ni $K\alpha\beta$	Cu $K\alpha\beta$	Zn $K\alpha\beta$
2.5	12.4	9.49	6.28	5.28	4.25
3	18.0	14.1	9.81	7.81	6.21
4	···	21.3	14.5	12.4	10.7
4.5	28.3	21.9	16.9	14.3	12.1
5	···	24.8	19.8	14.8	13.6
6	35.5	32.2	21.3	20.1	16.9
6.5	34.8	30.7	20.4	19.6	17.3
7	41.3	34.1	28.1	23.8	20.0
8	42.0	35.7	25.3	23.1	22.4
8.5	47.5	39.1	33.3	27.5	25.7
9	45.2	39.8	28.8	25.9	24.1
10	43.5	39.0	32.3	30.2	26.8
10.5	44.9	38.7	36.2	28.8	27.0
11	49.3	39.7	36.1	32.2	28.5
12	52.2	39.3	39.2	33.8	30.4

[a] Cross sections above were measured to a precision of 10% and an accuracy of 15%.

ANALYSIS AND RESULTS

The x-ray and particle spectra peaks were integrated by a computer program which subtracted

TABLE IV. *K* x-ray-production cross sections (b/sr).[a]

E (MeV)	Y	Mo	Ag	Cd
2.5	0.592	0.249	0.0856	0.0722
3	0.995	0.428	0.150	0.131
4	2.02	0.799	0.333	0.307
4.5	2.55	1.04	0.437	0.343
5	2.84	1.36	0.542	0.438
6	4.15	1.80	0.707	0.693
6.5	4.85	1.73	0.996	0.679
7	4.65	1.76	1.12	0.932
8	5.79	3.02	1.50	1.19
8.5	7.64	3.28	1.63	1.45
9	7.56	2.97	1.70	1.41
10	8.73	4.26	2.07	1.75
10.5	8.15	3.72	1.95	1.69
11	8.85	5.05	2.46	2.15
12	8.18	5.66	2.94	2.38

[a] Cross sections above were measured to a precision of 10% and an accuracy of 15%.

TABLE V. L x-ray-production cross sections (b/sr) for Lead.[a]

E (MeV)	$L\alpha$	$L\beta$	$L\gamma$
2.5	1.77	1.04	0.144
3	2.55	1.55	0.215
4	4.11	2.60	0.376
4.5	5.11	3.24	0.474
5	6.38	4.08	0.591
6	7.74	5.15	0.747
6.5	8.67	5.70	0.834
7	10.8	7.03	1.00
8	11.3	7.40	1.07
8.5	12.5	8.47	1.25
9	13.3	8.94	1.33
10	14.9	9.70	1.41
10.5	15.2	10.2	1.48
11	16.0	10.5	1.51
12	17.5	11.7	1.72

[a] Cross sections above were measured to a precision of 10% and an accuracy of 15%.

a linear background calculated from regions on either side of the peaks. The resulting x-ray yield was normalized to the beam and the mean target thicknesses given in Table II. The x-ray-production cross sections, corrected for detector efficiency, system absorption, dead time, and pileup, are given in Tables III–V.

The fluorescent yields of Table II (obtained from Ref. 21) were used to calculate K-shell ionization cross sections from the x-ray data. These numbers are shown in Figs. 3 and 4, plotted as a function of incident proton energy.

These results for Mn and Zn are consistent with those of Chaturvedi *et al.*[10] The data of Bissinger *et al.*[4] for Ni are also consistent, being 15–20% higher than the present values (even when corrected for new values of ω_K) for 5 and 8 MeV and within 5% at 11 MeV. The data of Bissinger *et al.*[7] for Ag is also consistent with the present data, but the differences are 15–25% between 2 and 6 MeV, and 1–14% between 8 and 12 MeV.

The recent data of Bearse *et al.*[9] are consistent with the present data for Ni at 2.5 MeV, Ag at 2.5 and 3 MeV, and Cu at 3 MeV. However, the data for Ni and Fe are more than a standard deviation away from the present data at 3 MeV.

The major errors in the present data lie in the efficiency determination and target thickness.

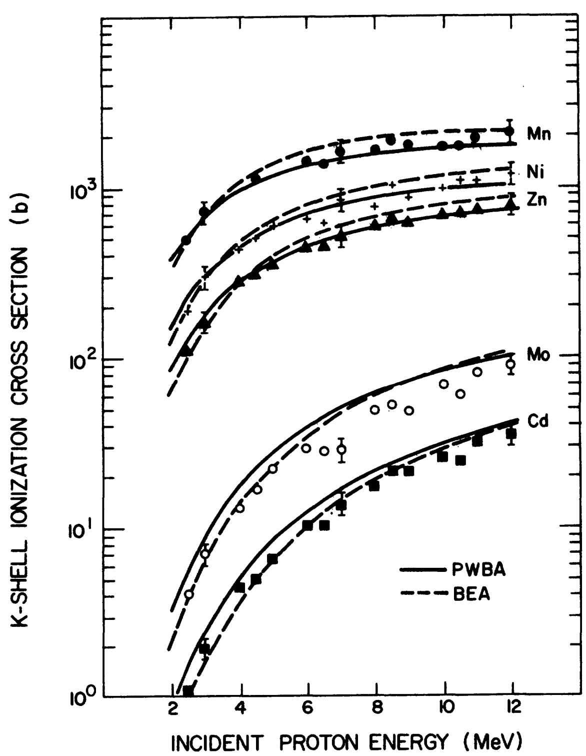

FIG. 3. K-shell ionization cross sections for Mn, Ni, Zn, Mo, and Cd as functions of the incident proton energy. PWBA calculations (solid line) and BEA calculations (broken line) are also shown.

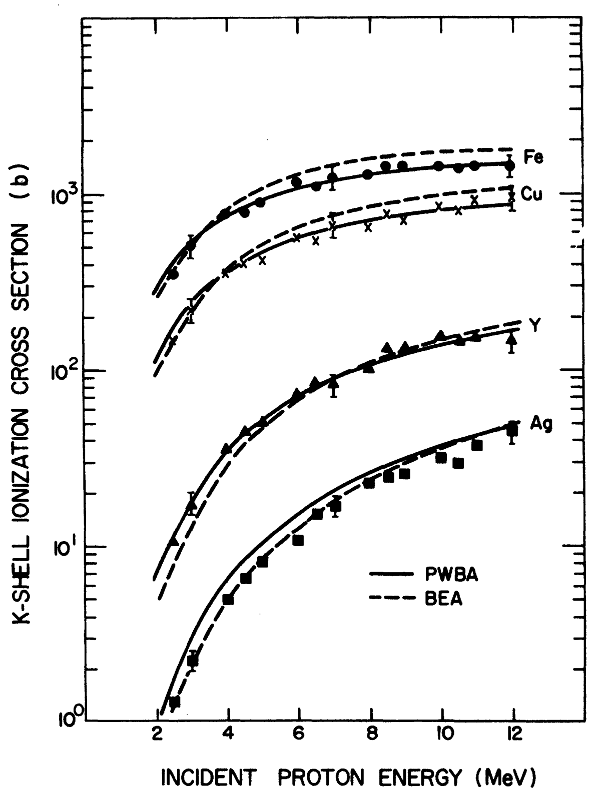

FIG. 4. K-shell ionization cross sections for Fe, Cu, Y, and Ag as functions of incident proton energy. The solid line represents PWBA calculations, while the broken line shows BEA predictions.

The estimated error is 5% and 10% in the relative and absolute efficiencies, respectively. Statistical errors were better than 1% for each run, and absorption corrections were made to 2%. The target-thickness measurement was limited by knowledge of the elastic scattering cross sections at 150°. The assumption of Rutherford scattering for some of the measurements is not likely to contribute substantially to disagreements with theory, since the discrepancies are worse for higher-Z targets, where the Rutherford assumption should be best. Also, for several of the targets, elastic scattering data were available at a number of energies (see Table II), and thicknesses extracted using this data were consistent to better than 7% with those extracted using Rutherford cross sections.

The data in Figs. 2 and 3 were fitted with the PWBA and BEA theories. The PWBA curve was obtained using the tables of Khandelwal *et al.*[24] with effective $Z_K = Z - 0.3$ and screening constant $\theta_K = I_K/Z_K^2 R_\infty$, where I_K is the K-shell ionization energy and R_∞ is the Rydberg constant. The BEA curves were obtained by scaling from the table given in Ref. 11. It is clear that the PWBA fits for atomic number below that of molybdenum are consistent with the data within experimental errors.

However, the BEA curves give a consistently better fit in the 2.5–4-MeV range for this Z region (25–39). For incident energies above 4 MeV, the BEA curves are systematically higher than the data, while the PWBA curve gives a better fit.

For the targets with Z higher than 41 (Mo, Ag and Cd), the PWBA fits no longer give an adequate fit to the data at energies under 10 MeV, while the BEA fits are excellent. The only exception to this trend is in the Mo data, where both theories are too high above 6 MeV incident energy.

In conclusion, it may be stated that the present data indicate that the BEA theory is more successful than the PWBA at incident energies below 4 MeV for the entire Z region studied, and between 4 and 11 MeV for Mo, Ag, and Cd. However, the PWBA gives better fits above 4 MeV for targets with Z between 25 and 39. It should be noted that the difference between the two theories is too small to allow a definitive choice to be made, because the errors in the measurements of these cross sections are still too high (10–15%). It is hoped that improved methods of detector-efficiency determinations will soon be available to improve this situation.

ACKNOWLEDGMENTS

The authors would like to thank R. Chaturvedi and J. Duggan for providing several of the radioactive sources needed for our efficiency measurements and the several undergraduates who helped with the more tedious work.

---

*Work supported in part by the U.S. Atomic Energy Commission.

†Present address: Nuclear Structure Research Laboratory, University of Rochester, Rochester, N.Y. 14627.

‡On leave from Institute "Ruder Bosković," Zagreb, Yugoslavia.

§Present address: Grand Valley State College, Allendale, Mich. 49401.

‖Present address: Institute "Ruder Bosković," Zagreb, Yugoslavia.

[1]E. Merzbacher and H. W. Lewis, in *Handbuch der Physik*, edited by S. Flügge (Springer-Verlag, Berlin, 1958), Vol. 34, p. 166.

[2]See, for example, J. D. Garcia, Phys. Rev. A 1, 280 (1970).

[3]See, for example, J. M. Hansteen and O. P. Mosebekk, Z. Phys. 234, 281 (1970).

[4]G. A. Bissinger, J. M. Joyce, E. J. Ludwig, W. S. McEver, and S. M. Shafroth, Phys. Rev. A 1, 841 (1970).

[5]O. N. Jarvis, C. Whitehead, and M. Shah, Phys. Rev. A 5, 1198 (1972).

[6]M. W. Lewis, B. E. Simmons, and E. Merzbacher, Phys. Rev. 91, 943 (1953).

[7]G. A. Bissinger, S. M. Shafroth, and A. W. Waltner, Phys. Rev. A 5, 2046 (1972).

[8]E. M. Bernstein and M. W. Lewis, Phys. Rev. 95, 83 (1954).

[9]R. C. Bearse, D. A. Close, J. J. Malanify, and C. J. Umbarger, Phys. Rev. A 7, 1269 (1973).

[10]R. Chaturvedi (private communication).

[11]J. D. Garcia, R. S. Fortner, and T. M. Kavanagh, Rev. Mod. Phys. 45, 111 (1973).

[12]C. A. Preskitt and W. P. Alford, Phys. Rev. 115, 389 (1959).

[13]V. Ya Golovnya, A. P. Klyucharev, B. A. Shilyaev, and N. A. Shlyakhov, Sov. J. Nucl. Phys. 4, 547 (1967).

[14]A. E. Antropov, S. I. Vasiliev, P. P. Zarubin, B. N. Orlov, A. V. Plavko, and A. I. Sorokin, Bull. Acad. Sci. USSR Phys. Ser. 34, 348 (1970).

[15]C. Mu, K. Kikuchi, S. Kobayashi, K. Matsuda, Y. Nagahara, Y. Oda, N. Takano, M. Takeda, and T. Yamazaki, J. Phys. Soc. Jap. 14, 865 (1959).

[16]L. L. Lee, Jr., and J. P. Schiffer, Phys. Rev. 134, B765 (1964).

[17]N. M. Mintz, Phys. Rev. 106, 1201 (1957).

[18]K. P. Lieb and T. Hausmann, Phys. Rev. 186, 1229 (1969).

[19]F. P. Brady, J. E. Draper, and J. A. McCray, Nucl. Phys. A 94, 449 (1967).

[20] A. E. Antropov, V. P. Bochin, P. P. Zarubin, B. N. Orlov, A. V. Plavko, and A. I. Sorokin, Bull. Acad. Sci. USSR Phys. Ser. 32, 1605 (1968).

[21] W. Bambynek, B. Crasemann, R. W. Fink, H.-U. Freund, H. Mark, C. D. Swift, R. E. Price, and P. Venugopala Rao, Rev. Mod. Phys. 44, 716 (1972).

[22] R. J. Gehrke and R. A. Lokken, Nucl. Instrum. Methods 97, 219 (1971).

[23] J. L. Campbell, P. O'Brien, and L. A. McNelles, Nucl. Instrum. Methods 92, 269 (1971).

[24] G. S. Khandelwal, B. M. Choi, and E. Merzbacher, At. Data 1, 103 (1969).